

EUROPEAN LABORATORY FOR PARTICLE PHYSICS

CERN-PPE/97-61

1 April 1997

THE VIRTUAL CATHODE CHAMBER

M. Capeáns, W. Dominik* , M. Hoch, L. Ropelewski, F. Sauli
(CERN, Geneva, Switzerland)

L. Shekhtman,
(BINP, Novosibirsk, Russia)

A. Sharma
(GRPHE, Université de Haute Alsace, Mulhouse, France)

ABSTRACT

We describe the operating principle and the first experimental results obtained with gas micro-strip detectors realized with anodes only on the active side, the multiplying field being provided from the back-plane and drift electrodes. For high rate operation, the detector has to be implemented on electron conducting supports, with resistivity around $10^{11} \Omega \text{ cm}$. By construction, the "Virtual Cathode Chamber" is not subjected to the possibility of discharges between anodes and cathodes, thus avoiding one of the most dangerous problems met with standard micro-strip chambers.

Submitted to Nuclear Instruments and Methods in Physics Research

* On leave of absence from Institute of Experimental Physics, University of Warsaw, Poland

1. INTRODUCTION

A grim problem encountered with Micro-Strip Gas Chambers (MSGCs) is the accidental onset of discharges between anode and cathode strips, leading to temporary inhibition of operation and to permanent damages to the strips [1]. The discharge probability can be strongly enhanced by simultaneous exposure of the detector to an intense radiation flux and to heavily ionizing tracks, such as those generated by nuclear interactions, neutrons or gamma conversions [2]. The process is understood to a result of the spontaneous transition of some avalanches from the proportional to the limited streamer regimes; a streamer generated in the high field region close to the dielectric support can then lead to a discharge [3]. The probability of the transition is a strong function of the operating voltage, and is enhanced by the higher surface field due to the presence of a resistive layer on the substrate, added to improve the rate capability of the detectors.

A direct solution of the problem is to remove altogether the cathodes from the detector side facing the gas, placing them on the back of the substrate; with a large potential applied on the back electrode, the electric field in the gas in the vicinity of anodes can be made strong enough and roughly reproducing the structure in a standard MSGC. In order to avoid accumulation of charges, a substrate with a moderate conductivity has to be used. This configuration was proposed many year ago, as an alternative to conventional wire chambers [4]; a new version with thin strips as electrodes, named "Coated Cathode Conductive Layer" (COCA COLA) chamber was introduced more recently, and its ability to obtain charge gain was demonstrated [5]. The material used for the support however (Tedlar¹) appeared to have a too high resistivity ($\sim 10^{15} \Omega \text{ cm}$) to effectively neutralize charges produced in the avalanches, and the operation of the detector was unstable even at low rates.

In this paper we present the results of measurements realized with two different detectors: a standard MSGC with cathodes not connected, emulating the cathode-less structure, and a new device having anode strips only on the active side, the electrodes on the back side of the substrate playing the role of cathodes in shaping an amplification field similar to the one of standard MSGCs.

An X-ray generator of controlled intensity delivering the 6 keV iron fluorescence line has been employed for the irradiation; all measurements have been performed with a gas filling of argon and dimethylether (DME) in equal proportions.

2. PRELIMINARY MEASUREMENTS

Pending the construction of a special, cathode-less micro-strip plate, we have emulated its operation using a standard MSGC with the cathodes not connected to a potential, named the "Floating Cathode Chamber" (FCC). This special type of operation has been independently studied by another author [6].

The MSGC used for the measurements had chromium anode and cathode strips, 7 and 100 μm wide respectively at 200 μm pitch, with an active area of 10 by

¹ Trade name of Du Pont de Nemours Co., Wilmington, Delaware (USA)

10 cm²; it was manufactured on 300 μm thick boro-silicate glass substrate² coated with a 50 nm thick Diamond-like Carbon (DLC) layer³ with a surface resistivity of $\sim 4 \cdot 10^{16} \Omega/\square$ [7]. The resistivity of the coating was tuned to this value by baking the MSGC plate at 250°C, following the procedure described in Ref. [8]. Three adjacent groups of anodes (16 strips wide each) were activated, with the two side groups grounded and the central ones connected to a charge sensitive amplifier followed by readout electronics. The wider strips, originally intended as cathodes, were connected to a common bus and left floating to imitate a cathode-less structure.

The detector was assembled with a rectangular, 3 mm thick polymer frame glued to the micro-strip plate, adding on the top a 300 μm thick glass plate made conductive on the inner side by gold evaporation and constituting the drift electrode. The back electrode was realized with a thin copper foil glued to an expanded polyurethane plate (Rohacell), and pressed to the outer surface of the micro-strip plate; no special care was taken to insure good electric contact between the surface of the glass and the electrode.

Under irradiation, the total current measured on the drift electrode corresponds to avalanches developing on all anode groups (an area 9.6 mm wide), while pulse height and rates were measured in the central group only. The irradiation flux was uniform within 20% over the exposed area of about 1.6 cm². Operational characteristics of the detector connected as a standard MSGC, with cathodes at negative potential, are described elsewhere [9].

Applying a high negative potential to the back plane, we observe a significant charge gain, around 1000 for -2650 V, at small radiation rates (25 Hz/mm², see Fig. 1). The amplitude distribution for avalanches on the central group is well separated from the noise; the low pulse height tail in the distribution is due to spurious pulses induced from the two adjacent groups of anodes, probably by capacitive coupling through the floating cathodes. As for a standard MSGC, the charge gain depends on the drift voltage, as shown in Fig. 2.

Use of a high resistivity ($\sim 3 \cdot 10^{15} \Omega \text{ cm}$) boro-silicate glass support seriously limits the rate capability of the detector (the presence of the DLC layer does not help in this configuration). Indeed, the static potential distribution on the detector surface is set by the current flowing between the back-plane electrode and the anode strips; ions produced in the avalanches and collected on the surface cause it to charge up, dynamically modifying the current density distribution. Because the leakage current, about 30 pA cm⁻², is comparable to the current of ions collected on the surface at rate of 50 Hz cm⁻² (at an avalanche size of $3 \cdot 10^5$ electrons), it is not surprising that the amplification process is rate dependent even at low rates. As shown in Fig. 3, the gain decreases by factor of 2 when the radiation rate is increased from 25 to 500 Hz/mm². The rate dependence of gain has as obvious consequence a rather poor energy resolution, although probably acceptable for a digital position-sensitive detector.

Note that the presence of the resistive thin layer, as well as the equipotentials constituted by the floating strips might have affected the operation, in particular concerning the distribution of the surface current and its effect on the field; the measurement is to be considered only an approximation to the final structure described in the next section.

² DESAG D-263: Low alkali boro-silicate glass made by Deutsche Spezialglass AG, Grünenplan (Germany)

³ Made by Plasma Assisted Chemical Vapor Deposition by SURMET Corp. Burlington, MA (USA)

3. THE VIRTUAL CATHODE CHAMBER

A real Virtual Cathode Chamber (VCC), with anode strips only on the gas side, has been realized on 300 μm thick electron-conducting glass⁴, with a volume resistivity of 10^{11} Ω cm, and an active size of 50 by 50 mm^2 (Fig. 4). A slightly diverging fan-like or “keystone” metal strip pattern (220 μm pitch on the bonding pad side and 200 μm at the opposite end) was engraved on one side⁵; strips were made of titanium, ~ 10 nm thick and 9 μm wide (this layer is normally used only to improve adhesion of thicker gold strips to the glass). The high resistance of the strips (>50 k Ω over 50 mm) and their non uniformity affected the measurements. The quality of artwork was also rather poor, and discontinuities in the strips could be expected. The detector was mounted with a drift electrode at 3 mm from the plane of the anode strips, using a mechanical assembly similar to the one described above. Strips were grouped by 7 on the bonding pads; the back side of the glass was coated with conductive varnish to form the back electrode. Negative potentials could be applied to the drift and to the back plane; one group of anode strips was connected to a charge amplifier, with two neighboring groups grounded through high value resistors. The X-ray beam from the generator was collimated on the central group of anodes, irradiating an area 10 mm long in the direction of the strips and 1.7 mm wide; the irradiated spot was fully contained within the group connected to the electronic readout.

Increasing the negative voltage applied to the back electrode above few hundred volts, pulses from avalanches induced by 6 keV X-rays are observed. The charge gain dependence on the back-plane potential, at fixed drift voltage, is shown in Fig. 5, measured at a rate of $4.3 \cdot 10^3$ Hz mm^{-2} ; the absolute gain is estimated from the avalanche current, measured on the drift electrode, taking into account the counting rate. Since only a fraction of the avalanche current is measured (part of the charge is removed by the substrate), this implies an underestimate, probably by a factor of two, of the real gain. The maximum voltage that could be applied to the back electrode was limited to around 1 kV by a significant increase of the leakage current, possibly due to defects in the glass surface.

The gain dependence on the back-plane voltage deviates from the standard exponential behavior expected from a simple Townsend mechanism of charge multiplication: a tendency to saturation at gains above 1000 is observed. The detector shows a rather poor energy resolution, presumably due to the already mentioned high resistivity of the strips, to the variable pitch in the irradiated area and to variations in the glass thickness.

The measurements of rate dependence of gain show good stability up to rates of about $3 \cdot 10^4$ Hz mm^{-2} for the highest charge gain (Fig. 6); the upper limit of gain stability moves towards higher rates for lower charge gains, demonstrating the dominant effect of the avalanche current in determining the gain. A theoretical limit on the rate capability can be estimated from simple considerations, assuming that, for a given drift voltage, the electric field in the gas in the vicinity

⁴ C85-1 glass produced by SSPC NIIES, Moscow, Russia.

⁵ VOSTOK, Novosibirsk, Russia

of the strips is defined by the potential distribution on the surface of the substrate. This is set by the voltage applied to the strips and by the current density in the substrate; positive ions produced in the avalanches and neutralized at the surface of the glass change the current in the substrate and affect the amplification field in the gas.

The current through the glass due to external charges can be approximated as $I=NQk$, where N is the avalanche rate per unit surface, Q the charge per avalanche and k the fraction of charge going to the surface. This current creates an additional local voltage drop dV across the glass, modifying the initial external field, given by:

$$dV = I\rho d = NQk\rho d;$$

where ρ and d are the bulk resistivity and the thickness of the substrate, respectively. As an example, for $\rho=10^{11}$ Ω cm, $d=0.03$ cm, $k=0.3$ (30% of positive ion current going to the surface) and $Q =3 \cdot 10^5$ electrons (6 keV X-ray conversions with gain 1000), $dV\sim 100$ V at $N\sim 3 \cdot 10^4$ Hz mm⁻². This implies that for a structure with the parameters listed above, the rate capability will be limited to $\sim 3 \cdot 10^4$ Hz mm⁻²; to achieve higher rate capabilities, use of a substrate with higher conductivity is mandatory.

4. CONCLUSIONS AND SUMMARY

In this preliminary work we demonstrate that a multi-anode structure, manufactured on electron-conducting glass with volume resistivity around 10^{11} Ω cm and with a moderate back plane potential, provides large enough gains to permit the efficient detection of radiation, and has sufficient rate capability for moderately high radiation environments. The principal advantage of the structure, named Virtual Cathode Chamber, is the suppression of any possibility of surface discharges between anodes and cathodes, severely limiting the use of standard MSGC at high gains in a high radiation flux. Saturation in the charge gain presumably makes the VCC less sensitive to the fluctuations of the primary ionization in gas due to heavily ionizing particles.

A Virtual Cathode Chamber manufactured on glass or plastic substrates with the required electrical and mechanical properties may be a solution for the realization of light, safe detectors of large size at moderate cost.

REFERENCES

- [1] R. Bouclier, M. Capeáns, C. Garabatos, G. Manzin, G. Million, L. Ropelewski, F. Sauli, T. Temmel, L. Shekhtman, V. Nagaslaev, Y. Pestov, and A. Kuleshov, *On some factors affecting the discharge conditions in micro-strip gas chambers*. Nucl. Instr. Methods **A365** (1995) 65.
- [2] B. Boimska, R. Bouclier, M. Capeáns, S. Claes, W. Dominik, M. Hoch, G. Million, L. Ropelewski, F. Sauli, A. Sharma, L. Shekhtman, W. VanDoninck, and L. VanLanker, *Study of ageing and gain limits of Microstrip Gas Chambers at high rates*, Proc. 5th Int. Conf. on Advanced Technology and Particle Physics, Como, October 7-11, 1996.
- [3] V. Peskov, B.D. Ramsey, and P. Fonte, *Surface Streamer Breakdown Mechanism in Microstrip Gas Counters*, Proc. Int. Conf. on Position Sensitive Detectors, Manchester, 9-13 September 1996.
- [4] M.J. Neumann and T.A. Nunamaker, *Modification of the Charpak Chamber with Foil Supported Conductors*, IEEE Trans. Nucl. Sci. **NS-17** (1970) 43.
- [5] R. Bouclier, J. Gaudaen, and F. Sauli, *The Coated Cathode Conductive Layer Chamber*, Nucl. Instr. Methods **A310** (1991) 74.
- [6] G. Cicognani, *Etude d'un Détecteur Gazeux à Micropistes avec Lecture à Pixels*. Thesis at Univ. Joseph Fourier, Grenoble (1997).
- [7] R. Bouclier, M. Capeáns, M. Hoch, G. Million, L. Ropelewski, F. Sauli, and T. Temmel-Ropelewski, *High rate operation of micro-strip gas chambers*, IEEE Trans. Nucl. Science **NS-43** (1995) 1220.
- [8] B.Boimska, R.Bouclier, M.Capeáns, W. Dominik, G. Million, L. Ropelewski, F. Sauli, A. Sharma, and T. Temmel-Ropelewski, *Progress with diamond over-coated micro-strip gas chambers*, Submitted to Nucl. Instr. Methods (1997) .
- [9] B. Boimska, R. Bouclier, W. Dominik, M. Hoch, G. Million, L. Ropelewski, F. Sauli, and A. Sharma, *Operation of Micro-Strip Gas Chambers manufactured on glass coated with high resistivity diamond-like layers*, Submitted to Nucl. Instr. Methods (1997) .

FIGURE CAPTIONS

Fig. 1: Pulse height spectrum for 6 keV X-rays recorded with the Floating Cathode Chamber made on DLC coated boro-silicate glass. The low amplitude peak corresponds to spurious signals induced from neighboring strips.

Fig. 2: Relative amplitude of the signal as a function of the voltage applied to the drift electrode.

Fig. 3: Dependence of the gain on the rate of avalanches for the floating cathodes detector.

Fig. 4: Schematics of the Virtual Cathode Chamber with an approximated representation of the electric field.

Fig. 5: Charge gain as a function of the back electrode voltage for the VCC manufactured of electron-conducting glass.

Fig. 6: Rate dependence of gain measured for three values of nominal charge gain with the VCC made on electron-conducting glass.

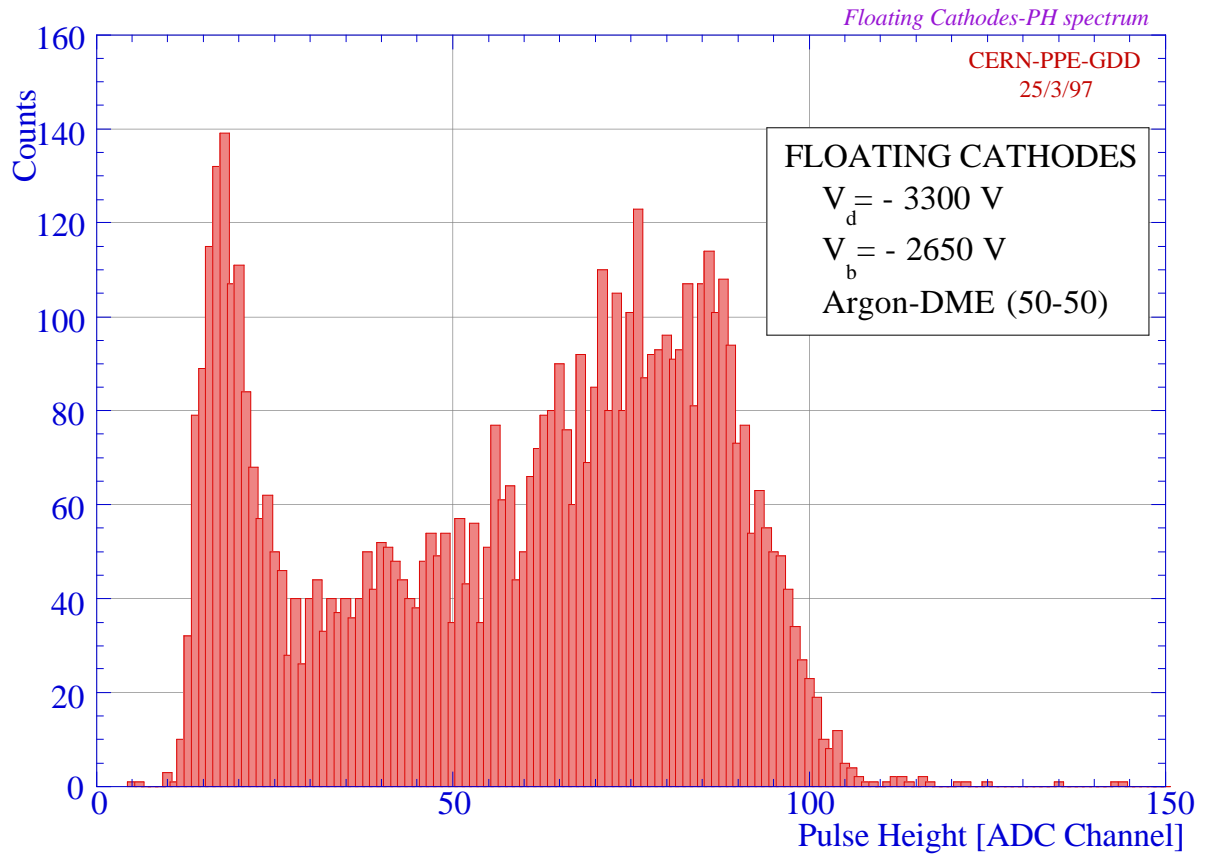


Fig. 1

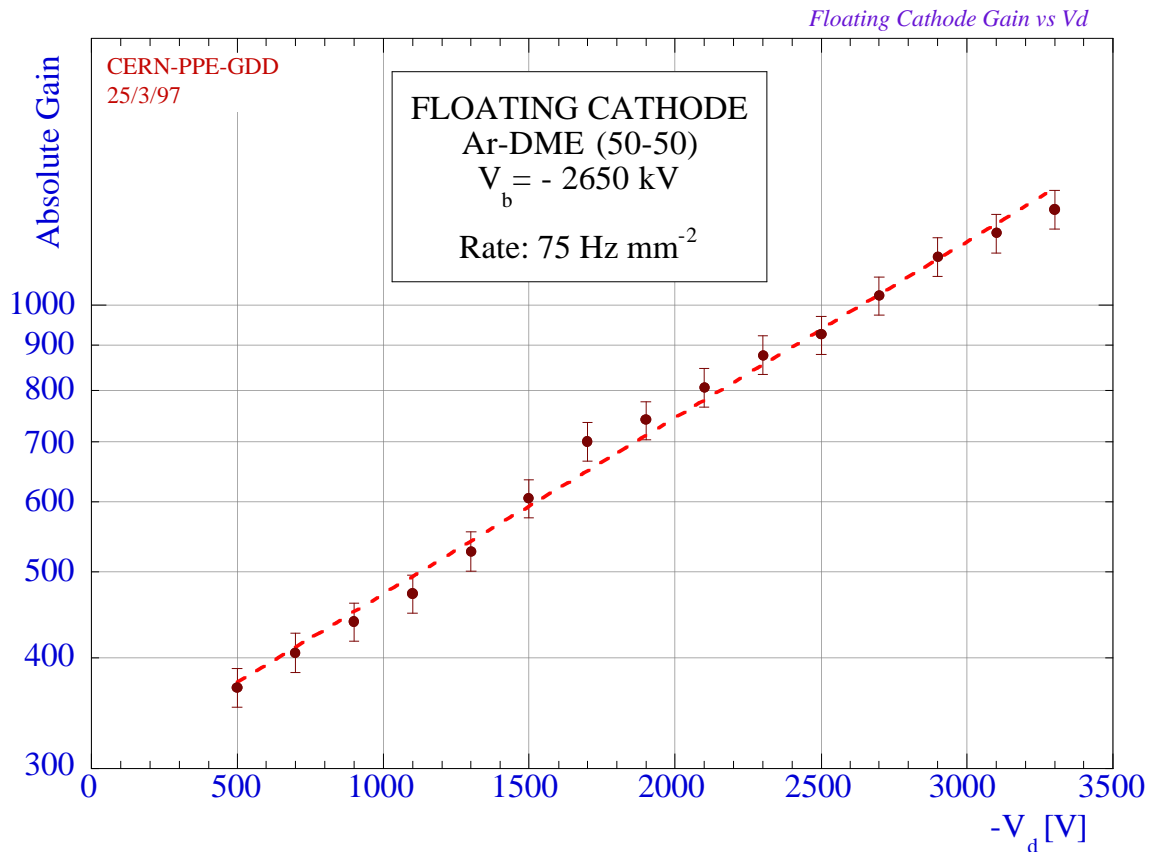


Fig. 2

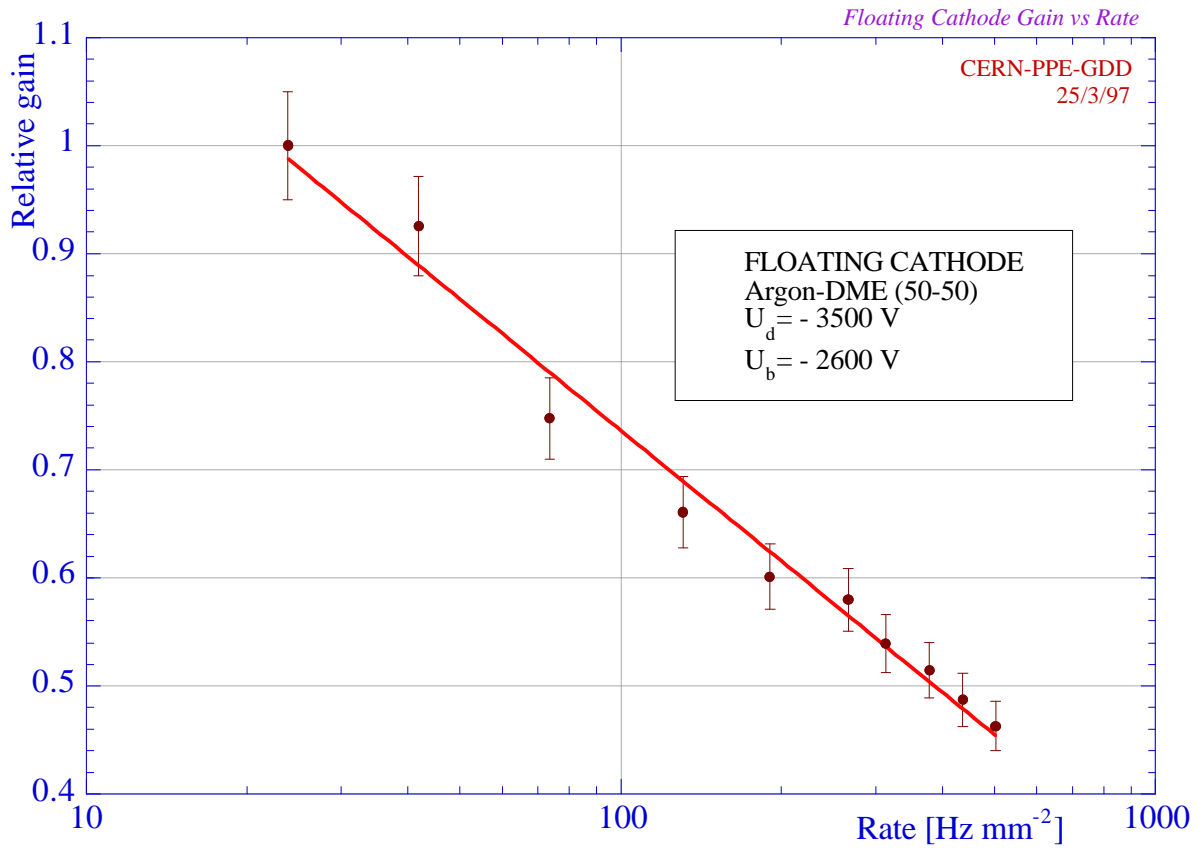


Fig. 3

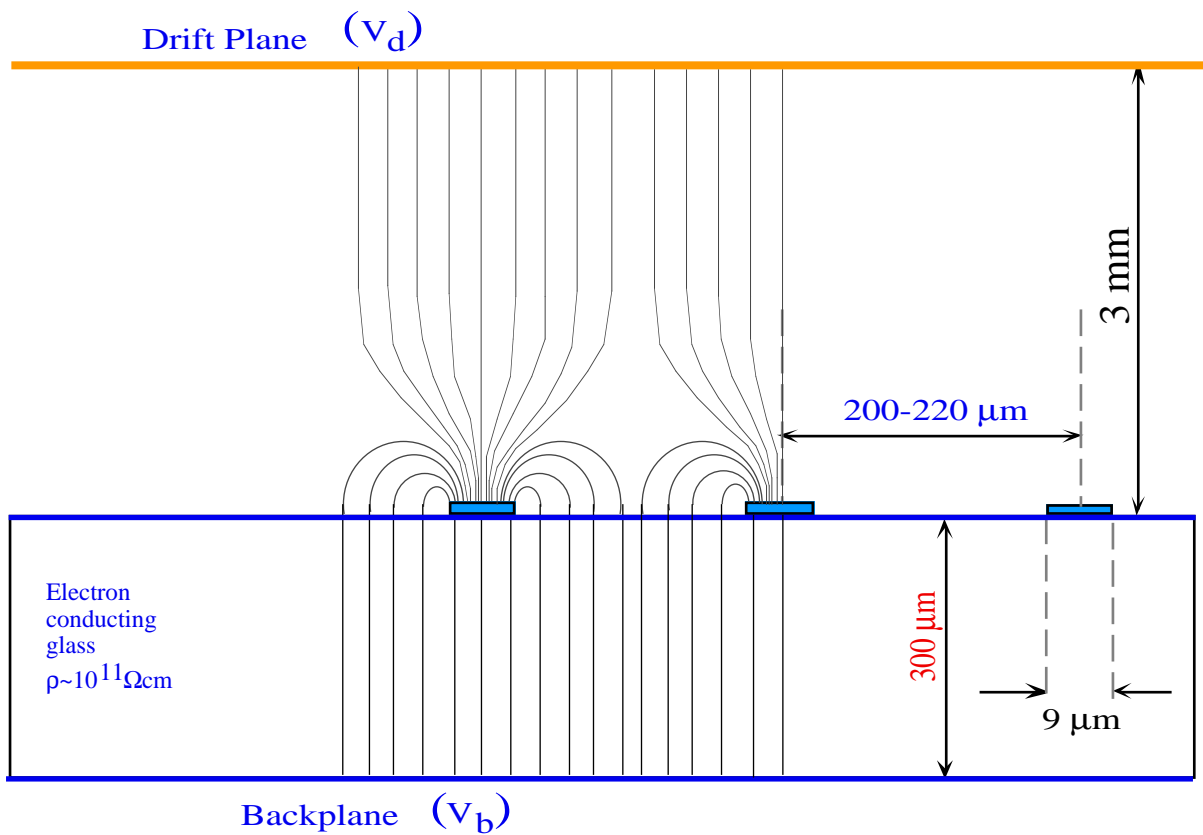


Fig. 4

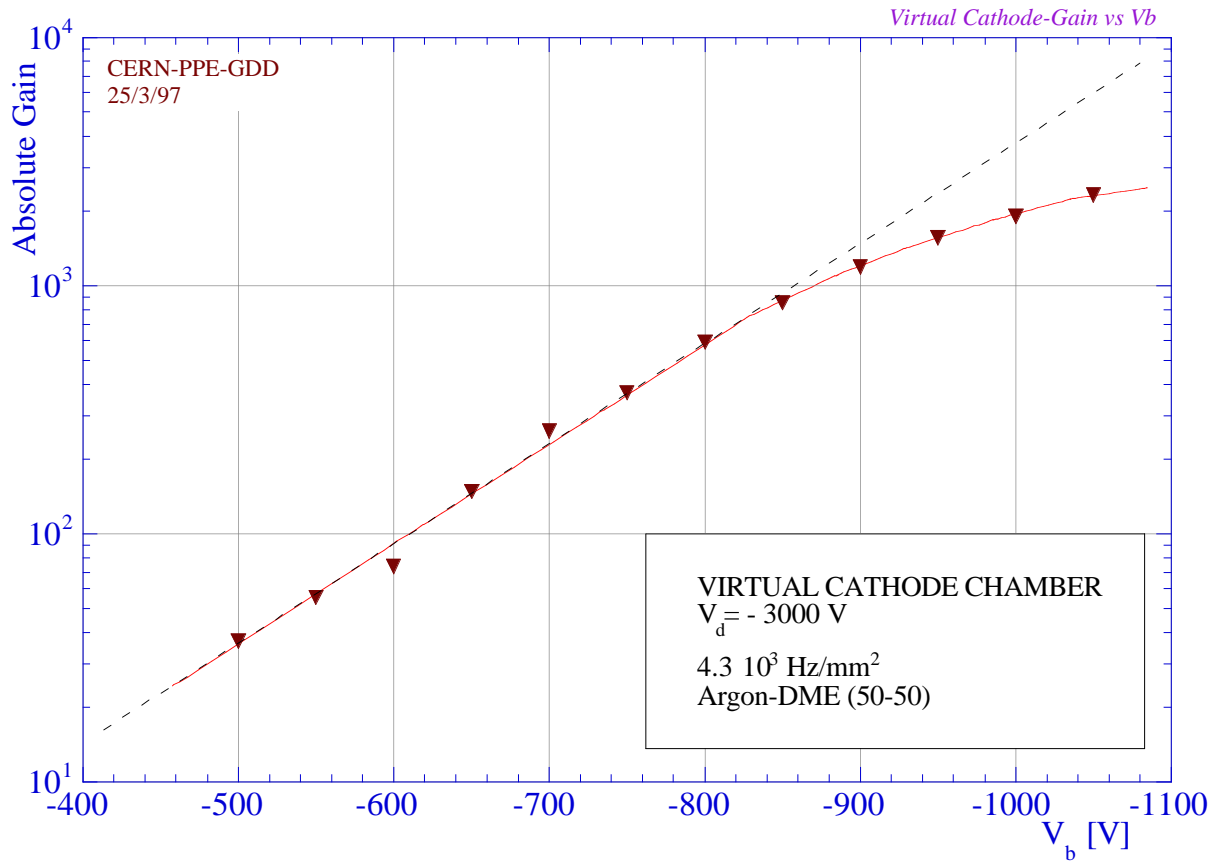


Fig. 5

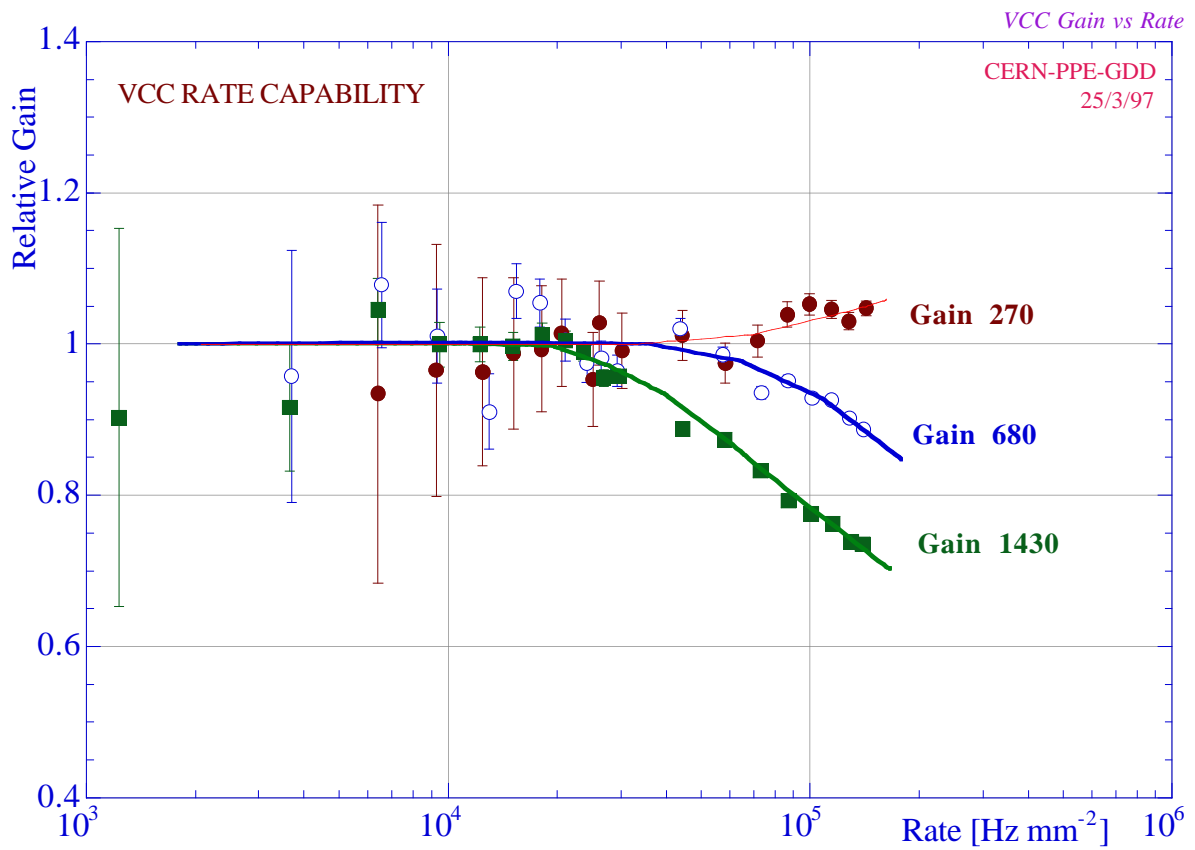


Fig. 6